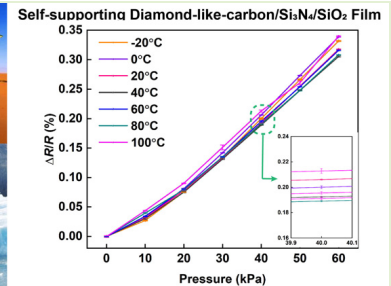
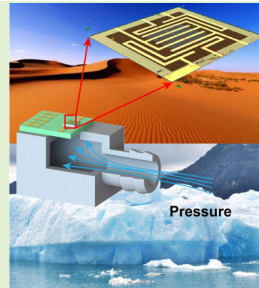


Self-Supporting Ultrathin DLC/Si₃N₄/SiO₂ for Micro-Pressure Sensor

Xin Ma, Qi Zhang, Peng Guo, Hao Li, Yulong Zhao, and Aiyong Wang

Abstract—In this study, we firstly reported a micro-pressure sensor based on self-supporting diamond-like carbon (DLC)/Si₃N₄/SiO₂ films with total thickness of 785 nm, where the DLC film was fabricated by a facile DC magnetron sputtering process. Particularly, the DLC film was selected as a hybrid sensitive and structural material due to its superior mechanical, piezoresistive properties and stability under harsh environment. Results showed that the sensitivity of the integrated sensor could reach $5.3 \times 10^{-5}/\text{kPa}$ within the pressure range of 0–60 kPa, together with the nonlinearity and the hysteresis was 5.7% FS (full scale) and 0.8% FS, respectively (at 20 °C). Most importantly, without any thermal insulation package, the sensitivity only changed slightly within $\pm 7.0\%$ even the temperature varied dramatically from $-20\text{ }^{\circ}\text{C}$ to $100\text{ }^{\circ}\text{C}$. Such excellent performance of the sensor was mainly originated from the good stability of atomic bond structure in DLC films, which was confirmed by the variable-temperature XPS test. In addition, the signal could be further compensated by the DLC thermal compensation resistor in which the temperature coefficient of resistance (TCR) was about $-1247.3\text{ ppm}/^{\circ}\text{C}$. These results bring forward a promising strategy to fabricate the micro-pressure sensor with high structural sensitivity, stability as well as lightweight design for micro-electromechanical system (MEMS) used in harsh applications.

Index Terms—Diamond like carbon, pressure sensor, piezoresistive, self-supporting film, MEMS.



I. INTRODUCTION

MICRO-ELECTROMECHANICAL system (MEMS) piezoresistive micro-pressure sensors have now been

Manuscript received November 9, 2021; revised December 1, 2021; accepted December 1, 2021. Date of publication December 8, 2021; date of current version February 28, 2022. This work was supported in part by the National Natural Science Foundation of China under Grant U20A20296 and Grant 51805425, in part by the Ningbo Science and Technology Innovation Project under Grant 2020Z023, and in part by the K. C. Wong Education Foundation under Grant GJTD-2019-13. The associate editor coordinating the review of this article and approving it for publication was Prof. Sang-Seok Lee. (Corresponding author: Qi Zhang.)

Xin Ma is with the State Key Laboratory for Mechanical Manufacturing Systems, School of Mechanical Engineering, Xi'an Jiaotong University, Xi'an 710049, China, and also with the Key Laboratory of Marine Materials and Related Technologies, Zhejiang Key Laboratory of Marine Materials and Protective Technologies, Ningbo Institute of Materials Technology and Engineering, Chinese Academy of Sciences, Ningbo 315201, China.

Qi Zhang and Yulong Zhao are with the State Key Laboratory for Mechanical Manufacturing Systems, School of Mechanical Engineering, Xi'an Jiaotong University, Xi'an 710049, China (e-mail: zhq0919@xjtu.edu.cn).

Peng Guo is with the Key Laboratory of Marine Materials and Related Technologies, Zhejiang Key Laboratory of Marine Materials and Protective Technologies, Ningbo Institute of Materials Technology and Engineering, Chinese Academy of Sciences, Ningbo 315201, China (e-mail: guopeng@nimte.ac.cn).

Hao Li and Aiyong Wang are with the Key Laboratory of Marine Materials and Related Technologies, Zhejiang Key Laboratory of Marine Materials and Protective Technologies, Ningbo Institute of Materials Technology and Engineering, Chinese Academy of Sciences, Ningbo 315201, China, and also with the Center of Materials Science and Optoelectronics Engineering, University of Chinese Academy of Science, Beijing 100049, China (e-mail: aywang@nimte.ac.cn).

Digital Object Identifier 10.1109/JSEN.2021.3133935

playing an increasingly important role in many industrial and medical applications, such as monitoring tiny pressure change for aviation, detecting intracranial and intraocular pressure for biomedical applications [1]–[3]. In particular, with rapid development of high-technique fields including deep-sea submersible, space exploration, clean nuclear energy system, it is of great necessary to fabricate the new sensitive materials and smart structures used in harsh environment, which can thereafter benefit the integrated MEMS micro-pressure sensors with high sensitivity, excellent stability, and facile process for lightweight manufacturing.

Nowadays, the size of the sensor chip is becoming more and more small, which requires the continuously reduced thickness of the sensitive structures [4]. However, one challenge is that fabricating ultra-thin films is rather difficult for traditional silicon-based process. Since the deep reactive ion etching (DRIE) process is significantly limited by the etching depth non-uniformity [5], and for epitaxy silicon process, preparing ultra-thin sensitive films also shows the disadvantages in complexity, equipment cost, and availability [6]. To overcome the above-mentioned issues, ultra-thin piezoresistive films based on advanced carbon materials have been attempted for micro-pressure sensors in view point of both structural and sensitive materials, such as graphene-BN [7], [8] and nanocrystalline diamond [9]. Nevertheless, the extremely high cost and the difficulties in mass fabrication for micro-pressure sensors is still an open barrier for their wide applications.

Recently, diamond-like carbon (DLC) films, belong to amorphous carbon family, have drawn much attention in MEMS

piezoresistive force, pressure and strain sensors [10]–[14], due to their superior physiochemical properties, unique piezoresistive effect with gauge factor (GF) from -3200 to 1200 [15]–[17], as well as the high compatibility with MEMS processes [18]. Moreover, if one keeps mind of the facile tailoring on thickness from monolayer [19] to over $50\text{-}\mu\text{m}$ [20], wide band gap of $1.0\text{--}4.0\text{ eV}$ [21] and high temperature stability ($300\text{--}500\text{ }^\circ\text{C}$) [22], [23], DLC films show strongly promising potential as an ultra-sensitive functional material for new micro-pressure sensors, especially serving in variable-temperature environment.

Very recently, we had fabricated several piezoresistive sensors based on various DLC films by utilizing the unique atomic bond structure and high residual stress in amorphous carbon matrix, and the piezoresistive mechanism of DLC films was basically discussed. The results also provided the facile combination method between the DLC films and traditional silicon-based or emerging flexible sensors [24]–[26]. However, to extend the application of DLC films based sensors, both the piezoresistive behavior and the new sensitive structures need to be further investigated, especially in harsh environment conditions.

In this work, we reported a unique self-supporting triple-layer structure for micro-pressure sensors to balance the sensitivity and structural stiffness, which included a 300 nm -thick SiO_2 film, a 285 nm -thick Si_3N_4 film and a 200 nm -thick DLC film from the bottom up. In particular, this nano-scale structure was designed to obtain high sensitivity and mechanical stability, and it could be easily fabricated using a simple process that based on the self-stop anisotropic etching. The sensitivity, stability, repeatability of the sensor within $-20\text{--}100\text{ }^\circ\text{C}$ were focused in terms of atomic bond evolution of DLC films.

II. DESIGN AND EXPERIMENT

A. Deposition of the DLC Film and Characterization Methods

The DLC film was deposited by a direct current (DC) magnetron sputtering technique with a graphite target of 99.9% purity. Four-inch $\text{Si}_3\text{N}_4/\text{SiO}_2/\text{silicon}$ wafers (n-type $\langle 100 \rangle$) were used as substrates. The base pressure was kept at $2.7 \times 10^{-3}\text{ Pa}$. Before deposition, all substrates were pre-cleaned by Ar^+ plasma glow. During film deposition, 65 sccm Ar gas was introduced to the target, with a work pressure of 0.3 Pa and a sputtering power of 2.1 kW . Additionally, in order to modify the ion energy, a pulsed -200 V bias voltage was applied to the substrates (350 kHz , $1.1\text{ }\mu\text{s}$, bipolar pulse). The deformation of the self-supporting film was investigated by a confocal microscope (OLS4000, Olympus). The atomic chemical bonds and the thermal stability of the DLC film was characterized by X-ray photoelectron spectroscopy with variable-temperature test function (XPS, Axis SUPRA). To clarify the performance of the sensor, a manual pump (JDQ-06S) was used to apply pressure load and it was calibrated by a piezometer (CWY100B), and desktop multimeter (Fluke 8846A) was used

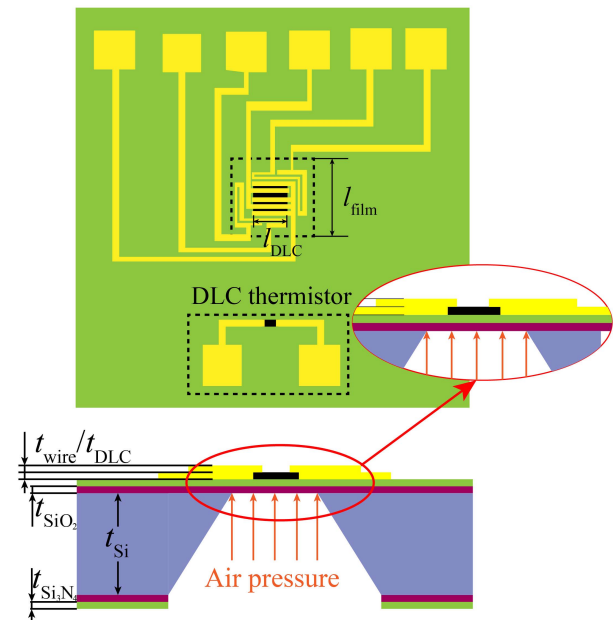


Fig. 1. Illustration of the micro-pressure sensor and the structure parameters, the inset figure is the enlarged view of the self-supporting film.

to record the electric signals. And the temperature, from $-20\text{ }^\circ\text{C}$ to $100\text{ }^\circ\text{C}$, was controlled by an oven (PSL-2J, Espec).

B. Design of the Micro-Pressure Sensor

Here, a classical flat-film structure was used for the convenience in sensor fabrication. Fig. 1 shows the designed DLC/ $\text{Si}_3\text{N}_4/\text{SiO}_2$ self-supporting film structure with sub-micron thickness. The full size of the chip was $3.0\text{ mm} \times 3.0\text{ mm} \times 0.5\text{ mm}$, where the dimension of the DLC film was $250\text{ }\mu\text{m} \times 250\text{ }\mu\text{m}$ (l_{DLC}). And the dimension of the sensitive structure film was $500\text{ }\mu\text{m} \times 500\text{ }\mu\text{m}$ (l_{film}). The total thickness ($t_{\text{DLC}} + t_{\text{SiO}_2} + t_{\text{Si}_3\text{N}_4}$) of the self-supporting film was only about 785 nm ($200\text{ nm DLC}/285\text{ nm Si}_3\text{N}_4/300\text{ nm SiO}_2$). Therefore, the ratio of width/thickness reached up to about 637 , which made the structure very sensitive. And the DLC film was set on the stress concentration area to further improve the sensor's sensitivity. In addition, the dimensions of the thermal compensation resistor were set at $20 \times 20\text{ }\mu\text{m}$. The DLC film was designed on the center of the sensitive structure for the distribution of the stress and the heat dissipation. And auxiliary metal wires were added on the self-supporting film to conduct the heat.

Since the accurate analytical expression of the pressure-stress relation has not been gained yet for such a thin rectangular film structure, due to the nonlinear phenomenon. We used finite element method (FEM, COMSOL Multiphysics) to study the quality of the output signal and stress distribution. In our previous work [25], DLC piezoresistive material had been added into the system material library. Noted that the GF of the DLC film in this work was 2.98 , which was measured by a three-point testing method. Usually, the GF had a close relationship with the sp^2 phase content [24]. In this work, its higher sp^2 content may cause a smaller GF [17], [27].

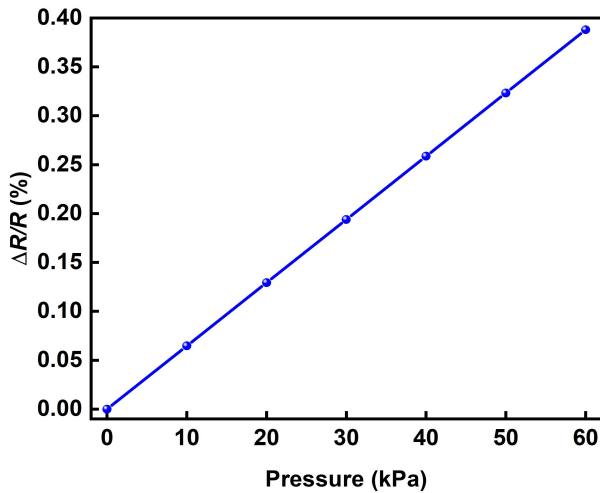


Fig. 2. The fitted output resistance signal of the sensor with applied pressure.

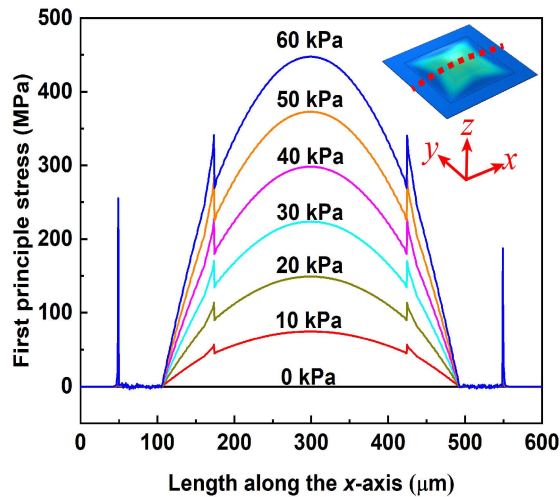


Fig. 3. First principle stress along the center line of the surface within pressure load of 0-60 kPa, the inset figure shows the typical distribution of the stress at 60 kPa, in which the red dash line is the center of the surface of the self-supporting film.

During simulation, the pressure of 0-60 kPa with interval of 10 kPa was applied onto the backside of the self-supporting film. As shown in Fig. 2, the resistance signal $\Delta R/R$ increased linearly with the applied pressure, in which its average sensitivity was about $6.46 \times 10^{-5}/\text{kPa}$. The inset figure of Fig. 3 showed the uniform distribution of the first principle stress on the center area of this square sensitive film. Moreover, the first principle stress of the typical line (red dash line, the center of the surface of the self-supporting film) increased uniformly as the pressure increased, and the maximum stress was about 447 MPa, as shown in Fig. 3.

The coefficient of thermal expansion (CTE), heat capacity at constant pressure (C_p), and coefficient of thermal conductivity (λ) of these films are different, which are shown in Table I. Considering the thermal stress could not be avoided in the triple-layer structure when the environment temperature changes, we also studied the stress evolution as a function of temperature by FEM, the maximum thermal stress about

TABLE I
THERMAL PARAMETERS OF MATERIALS

Materials	CTE (K ⁻¹)	C _p (J·kg ⁻¹ ·K ⁻¹)	λ (W·m ⁻¹ ·K ⁻¹)
Silicon	2.6E-6	700	130
SiO ₂	0.5E-6	730	1.4
Si ₃ N ₄	2.3E-6	700	20
DLC[28-30]	2.3E-6	800	1

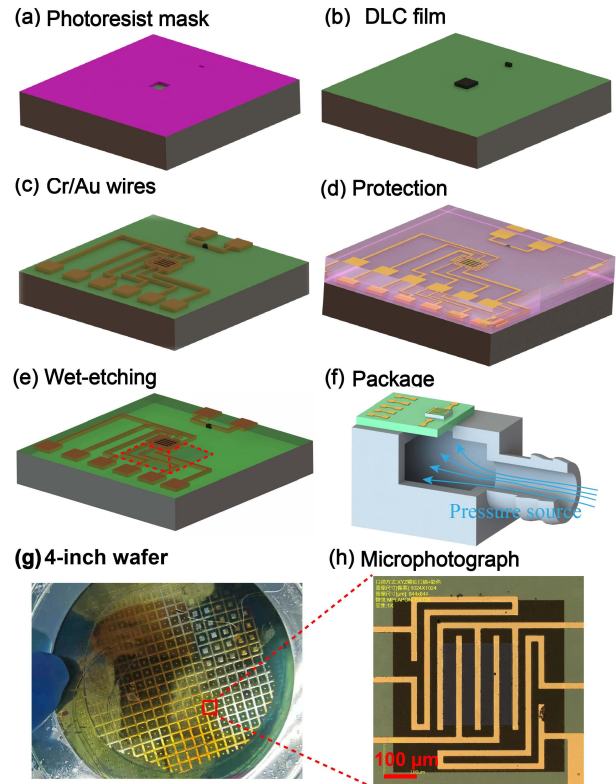


Fig. 4. Schematic of the fabrication and package processes and the microphotograph of the sensor. (a) Using photoresist as mask during the low-temperature deposition process. (b) Fabricating DLC resistors. (c) Electrical connection. (d) Protecting sensitive components with photoresist/PDMS/glass. (e) Fabricating the cavity using wet etching process. (f) Packaging with PCB board and 3D printed shell. (g) 4-inch wafer after the fabrication process. (h) Microphotograph of the self-supporting sensitive film and the DLC piezoresistive film, the thermal compensation resistor was not shown here (the dimensions of the sensitive film were not in strict conformance with the design values, since the thickness of the silicon substrate had a fabrication error).

27 MPa was obtained at $-20\text{ }^\circ\text{C}$, which was much smaller than that caused by the applied pressure. Additionally, the effect of the thermal stress can also be eliminated by the thermal compensation.

C. Fabrication of the Micro-Pressure Sensor

Subsequently, the designed sensor chips were fabricated using a double side polished 4-inch (n-type (100)) silicon wafer. The thickness of it was $500\text{ }\mu\text{m}$, with 285 nm-thick Si₃N₄ film and 300 nm-thick SiO₂ film on both sides, which were used for the self-stopping wet etching process and as insulation between DLC films and silicon substrate. Because the deposition temperature of DLC films was controlled below $50\text{ }^\circ\text{C}$, the photoresist (EPG 535) could be directly

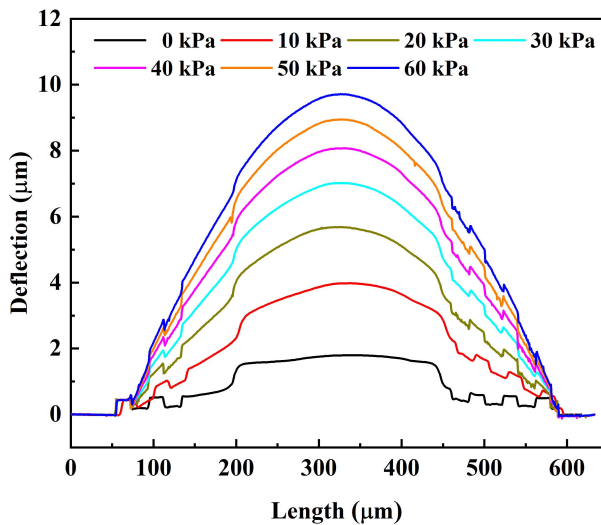


Fig. 5. The deflection curves under the pressure load within 0-60 kPa.

used as mask, as shown in Fig. 4(a). After this process, DLC film was deposited by a traditional DC magnetron sputtering process shown in Fig. 4(b). Then, patterned DLC piezo-resistors were fabricated using lift-off process. As shown in Fig. 4(c), a 20 nm-thick Cr film and 200 nm-thick Au film were subsequently deposited to fabricate wires and electrodes. To fabricate the mask for wet etching, the SiO₂ and Si₃N₄ films on the bottom side were selectively removed by inductively coupled plasma (ICP) etching. Then, from bottom to top, the components on the front side were carefully protected by photoresist, PDMS and glass (Fig. 4(d)). Next, wet etching process was carried out under 90 °C with the KOH etchant of a mass fraction of 33% to generate the cavity, when the silicon was etched over and the final self-supporting structure of 785 nm-thick was obtained finally, as shown in Fig. 4(e). In Fig. 4(f), the sensor chip was further pasted onto PCB board using silicone rubber, and then fixed onto a 3D printed shell with a cavity inside. With this simple and economical process, the mass fabrication of the DLC based micro-pressure sensor was firstly realized (Fig. 4(g)), which showed the very strong competitiveness in industrial field. Noted that the release of the initial high compressive stress in DLC might cause wrinkles in this ultra-thin sensitive structure [31], [32], and in this work, a smaller area of DLC film was deposited to obtain a flat surface. Additionally, thinner DLC film or DLC film with smaller initial stress could also solve the problem, but the loss of the piezoresistive performance should also be taken into consideration.

III. EXPERIMENTAL RESULTS

A. Characterization of the Deflections

The deflections of the self-supporting film with applied pressure 0-60 kPa were characterized by confocal microscope. As shown in Fig. 5, the self-supporting sensitive film had a flat surface (the ups and downs of the surface caused by the wires and the edge of the DLC film was enlarged in this figure), and the maximum deflection was approximately 1.8 μm. When the pressure was lower than 20 kPa, the self-supporting film

was not completely swelled for the edges of the DLC film, which might cause the loss of the sensitivity. Beyond 20 kPa, the maximum deflection varied from 5.7 μm to 9.7 μm, and the edges of the DLC film were almost disappeared. The appearance of this film was very closer to an ideal flat surface. Therefore, it could be supposed that the sensitivity of the sensor might be had a little decrease when the pressure was lower than 20 kPa, while its performance would stabilize and be improved in the range of 20-60 kPa.

B. Characterization of the Thermal Stability by Variable-Temperature XPS Test

Before evaluating the sensor performance under variable temperature, the internal stability of the DLC film was investigated by the variable-temperature XPS method. Fig. 6(a) displays the typical amorphous C 1s spectra of the DLC film within the temperature range of -20 °C~100 °C. Generally, it is empirically known that the C 1s spectra of DLC films can be separated into peaks at 284.6 eV and 285.4 eV, which is assigned to the sp² hybridization (C=C) and sp³ hybridization (C-C), respectively. In addition, the C-O/C=O peaks around 286.5 eV also existed in all C 1s spectra and the oxygen content was mostly below 4.0 at. %, which was resulted from the residual oxygen in chamber during DLC deposition. As the temperature varied from -20 °C to 80 °C, the fitted results in Fig. 6(b) showed that both the sp² and sp³ contents kept stable in the range of 38.0 ± 1.1% and 62.0 ± 1.1%, respectively. However, the slight decrease to 57.5% for sp² content and increase to 42.5% for sp³ content were obtained, when the temperature reached to 100 °C. This could be attributed to the increase of oxygen content up to 7.6 at. % at this temperature for the decrease of vacuum degree, which affect the in-situ measurement of atomic carbon bond (Fig. 6(c)). As a result, it could be said that such hydrogen-free DLC film showed the advantage of good thermal stability within temperature range of -20 °C~100 °C.

C. Performance of the Micro-Pressure Sensor

In the variable-temperature test, the micro-pressure sensor was put into an oven and the chamber temperature was controlled within -20~100 °C with the interval of 20 °C, with fluctuation about ±0.1 °C, which was shown in Fig. 7. Inside the chamber, a protection cover without heat insulation function was used to cut off the airflow disturbance. The pressure was controlled within 0-60 kPa with an interval of 10 kPa.

Fig. 8(a) shows the signal of the thermal compensation resistor, where the TCR was about -1247.3 ppm/°C and this good linearity made great contribution to the subsequent signal compensation. For the TCR is important to piezoresistive sensors, so a comparison is listed in Table II. The TCR of DLC is usually negative but can be adjusted to zero or positive by metal doping. Compared with other materials in the table, it is more flexible to adjust the TCR of DLC. As shown in Fig. 8(b), the sensitivity at 20 °C was about 5.3 × 10⁻⁵ kPa⁻¹, which agree well with the simulated result by FEM. Within the pressure range of 0-60 kPa, the

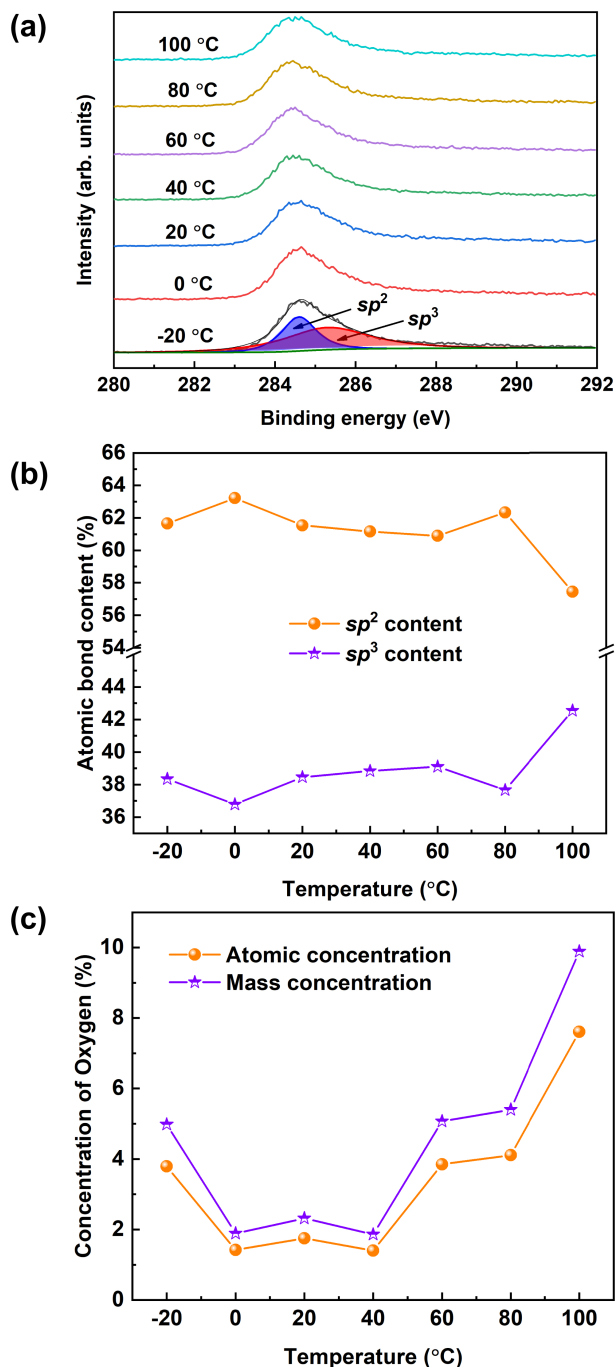


Fig. 6. Variable-temperature XPS test result. (a) The original data at variable temperature and the fitted sp²/sp³ peaks at -20 °C. (b) The contents of sp²/sp³ phases. (c) Concentration of oxygen under -20~100 °C.

sensor performed a good linearity performance, where the nonlinearity and hysteresis of the signal was only 5.7% FS and 0.8% FS, respectively. Fig. 8(c) exhibits the temperature stability under variable temperature condition. Without any heat insulation package or compensation, the sensitivity of the sensor only varied slightly within ±7.0% in the temperature range of -20~100 °C, comparing to the sensitivity at 20 °C as a benchmark. The error bar in the inset figure of Fig. 8(c) demonstrated the very tiny signal variation, during the 30 s' loading pressure stage. Moreover, the sensor displayed the good repeatability after the 500 cycles test shown in Fig. 8(d).

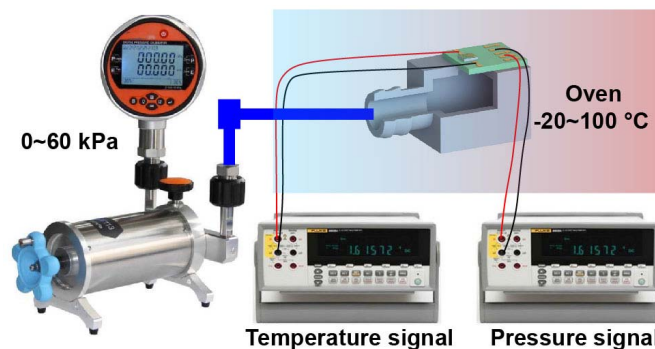


Fig. 7. The illustration of the variable temperature test system for the sensor.

TABLE II
COMPARISON OF TCR BETWEEN RELATED WORKS

Refs.	TCR
Graphene[33, 34]	2480-110000 ppm/°C
SiC[35, 36]	-(3500-7508) ppm/°C
Ni-Cr film[37]	18-253 ppm/°C
Doped single crystal silicon[38]	250-2699 ppm/°C
DLC(Me: DLC)[39-41]	-408-39000 ppm/°C
DLC (this work)	-1247.3 ppm/°C

TABLE III
COMPARISON OF THE SENSITIVITY, THICKNESS AND PROCESSES BETWEEN RELATED WORKS

Refs.	Normalized sensitivity	Thickness	Fabrication process
Silicon[42]	3.6×10 ⁻⁵ /kPa	2 μm	SOI + ion doping + etching
Polysilicon[43]	2.896×10 ⁻⁵ /kPa	6.3 μm	PECVD + ion doping + etching + sealing
Graphene[8]	2.97×10 ⁻⁵ /kPa	0.335 nm	Manual transfer
Nanocrystalline diamond[9]	6×10 ⁻⁵ /kPa	150 nm	MPECVD (550 °C) + etching
DLC (this work)	5.3×10 ⁻⁵ /kPa	645 nm	DC sputtering (50 °C) + etching

The sensor also exhibited the good repeatability at low/high temperature, as shown in Fig. 9.

Compared with traditional materials based sensors, such as silicon and polysilicon, the sensitivity performance of the DLC based sensor is better, and the fabrication process of the DLC based sensors is easier and more economical, which is shown in Table III. Noted that the units of related works (bar/mmHg) were converted into "kPa." Compared with previous related works on graphene and nano-crystalline diamond, both the performance and the facile fabrication process of the present micro-pressure sensor based on DLC/Si₃N₄/SiO₂ give great promising advantages. For example, when the suspended 0.335 nm-thick graphene and 150 nm-thick nano-crystalline diamond film was used as sensitive material and structure, the normalized sensitivity was 2.97 × 10⁻⁵/kPa and 6 × 10⁻⁵/kPa, respectively. The sensitivity of these sensors was at the similar level with this work. But the sensitive structure of this work is much thicker, which means lower structure

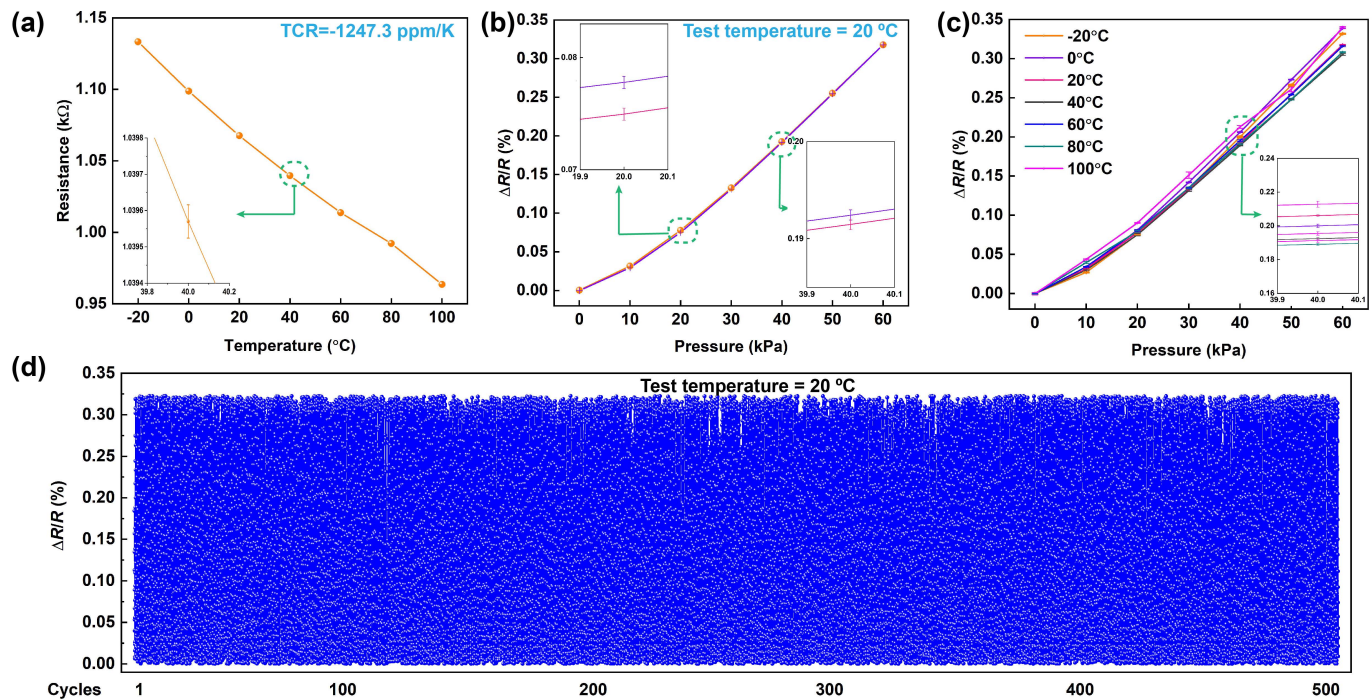


Fig. 8. Test results of the DLC micro-pressure sensor, which shows the good linearity, repeatability, and temperature stability performances. (a) The relation of the resistance and temperature of the DLC thermal compensation resistor. (b) The output signal of the pressure sensitive resistor under loading and unloading procedures. (c) Variable temperature performance of the sensor within the range of -20 to 100 °C. (d) The repeatability result of the sensor with 500 cycles.

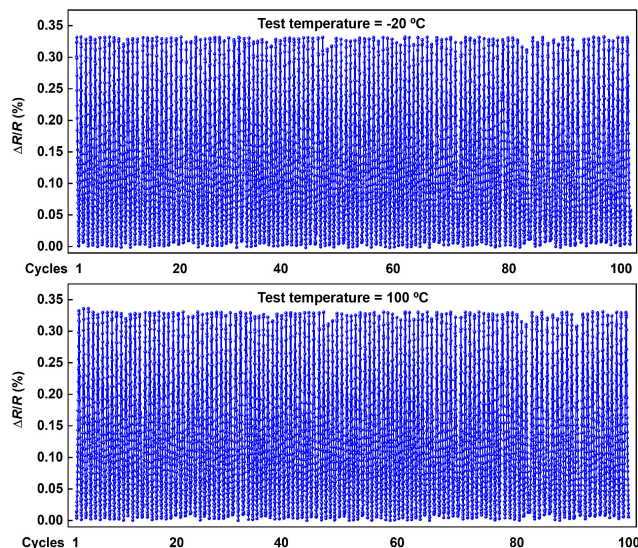


Fig. 9. The repeatability result of the sensor at -20 and 100 °C with 100 cycles.

sensitivity, better stiffness and linearity performance. Most importantly, the DLC film was directly deposited on the silicon wafer using a traditional DC magnetron sputtering technique at low-temperature, which benefit the facile fabrication, uniform over large area, and the excellent manufacturing compatibility to current industrial MEMS processes.

IV. CONCLUSION

In conclusion, a high-performance MEMS micro-pressure sensor based on ultra-thin DLC/ $\text{Si}_3\text{N}_4/\text{SiO}_2$ was designed and

fabricated successfully. Taking the advantage of piezoresistive behavior of DLC film and the thin self-supporting structure, the sensitivity of the integrated sensor was elevated up to $5.3 \times 10^{-5}/\text{kPa}$, together with a good nonlinearity of 5.7% FS and a small hysteresis of 0.8% FS, as well as good repeatability. Most important result was that the sensitivity of the sensor behaved a good thermal stability with slight variation within $\pm 7.0\%$ as the temperature change from -20 °C to 100 °C. According to the variable-temperature XPS test, the high performance of the sensor was mainly attributed by the superior stability of sp^2/sp^3 atomic bond in DLC films. In addition, the thermal compensation resistor with a stable TCR of -1247.3 ppm/°C made another contribution for further signal quality elevation. It could be concluded that these results not only provide new insight into the thermal performance of DLC piezoresistive sensor, but also bring forward to the new promising strategy to design and fabricate the micro-pressure sensor with high structural sensitivity, stability and repeatability as well as facile processing for harsh environment.

REFERENCES

- [1] X. Meng and Y. Zhao, "The design and optimization of a highly sensitive and overload-resistant piezoresistive pressure sensor," *Sensors*, vol. 16, no. 3, p. 348, Mar. 2016, doi: [10.3390/s16030348](https://doi.org/10.3390/s16030348).
- [2] T. Xu *et al.*, "Piezoresistive pressure sensor with high sensitivity for medical application using peninsula-island structure," *Frontiers Mech. Eng.*, vol. 12, no. 4, pp. 546–553, Dec. 2017, doi: [10.1007/s11465-017-0447-9](https://doi.org/10.1007/s11465-017-0447-9).
- [3] T. Guan *et al.*, "A novel 0–3 kPa piezoresistive pressure sensor based on a shuriken-structured diaphragm," in *Proc. IEEE 29th Int. Conf. Micro Electro Mech. Syst. (MEMS)*, Jan. 2016, pp. 816–819, doi: [10.1109/memsys.2016.7421754](https://doi.org/10.1109/memsys.2016.7421754).

- [4] S.-C. Gong and C. Lee, "Analytical solutions of sensitivity for pressure microsensors," *IEEE Sensors J.*, vol. 1, no. 4, pp. 340–344, Dec. 2001, doi: [10.1109/7361.983474](https://doi.org/10.1109/7361.983474).
- [5] D. Jiao, Z. Ni, J. Wang, and X. Li, "Ultra-small pressure sensors fabricated using a scar-free microhole inter-etch and sealing (MIS) process," *J. Micromech. Microeng.*, vol. 30, no. 6, Jun. 2020, Art. no. 065012, doi: [10.1088/1361-6439/ab8909](https://doi.org/10.1088/1361-6439/ab8909).
- [6] A. A. Barlian, W.-T. Park, J. R. Mallon, Jr., A. J. Rastegar, and B. L. Pruitt, "Review: Semiconductor piezoresistance for microsystems," *Proc. IEEE*, vol. 97, no. 3, pp. 513–552, Mar. 2009, doi: [10.1109/JPROC.2009.2013612](https://doi.org/10.1109/JPROC.2009.2013612).
- [7] M. Li *et al.*, "Pressure sensing element based on the BN-graphene-BN heterostructure," *Appl. Phys. Lett.*, vol. 112, no. 14, Apr. 2018, Art. no. 143502, doi: [10.1063/1.5017079](https://doi.org/10.1063/1.5017079).
- [8] A. D. Smith *et al.*, "Electromechanical piezoresistive sensing in suspended graphene membranes," *Nano Lett.*, vol. 13, no. 7, pp. 3237–3242, Jul. 2013, doi: [10.1021/nl401352k](https://doi.org/10.1021/nl401352k).
- [9] S. D. Janssens, S. Drijkoningen, and K. Haenen, "Ultra-thin nanocrystalline diamond membranes as pressure sensors for harsh environments," *Appl. Phys. Lett.*, vol. 104, no. 7, Feb. 2014, Art. no. 073107, doi: [10.1063/1.4866028](https://doi.org/10.1063/1.4866028).
- [10] S. Biehl, C. Rumposch, G. Bräuer, H.-W. Hoffmeister, and M. Luig, "Development of a novel piezoresistive thin film sensor system based on hydrogenated carbon," *Microsyst. Technol.*, vol. 20, nos. 4–5, pp. 989–993, Apr. 2014, doi: [10.1007/s00542-014-2101-3](https://doi.org/10.1007/s00542-014-2101-3).
- [11] E. Peiner, A. Tibrewala, R. Bandorf, H. Lüthje, L. Doering, and W. Limmer, "Diamond-like carbon for MEMS," *J. Micromech. Microeng.*, vol. 17, no. 7, pp. S83–S90, Jul. 2007, doi: [10.1088/0960-1317/17/7/s04](https://doi.org/10.1088/0960-1317/17/7/s04).
- [12] P. Xue, C. Chen, and D. Diao, "Ultra-sensitive flexible strain sensor based on graphene nanocrystallite carbon film with wrinkle structures," *Carbon*, vol. 147, pp. 227–235, Jun. 2019, doi: [10.1016/j.carbon.2019.03.001](https://doi.org/10.1016/j.carbon.2019.03.001).
- [13] S. Uhlig, H. Schmid-Engel, T. Speicher, and G. Schultes, "Pressure sensitivity of piezoresistive nickel-carbon Ni:a-C: H thin films," *Sens. Actuators A, Phys.*, vol. 193, pp. 129–135, Apr. 2013, doi: [10.1016/j.sna.2012.12.027](https://doi.org/10.1016/j.sna.2012.12.027).
- [14] R. Kometani, K. Yusa, S. Warisawa, and S. Ishihara, "Piezoresistive effect in the three-dimensional diamondlike carbon nanostructure fabricated by focused-ion-beam chemical vapor deposition," *J. Vac. Sci. Technol. B, Nanotechnol. Microelectron., Mater., Process., Meas., Phenomena*, vol. 28, no. 6, pp. C6F38–C6F41, Nov. 2010, doi: [10.1116/1.3504584](https://doi.org/10.1116/1.3504584).
- [15] Š. Meškinis *et al.*, "Giant negative piezoresistive effect in diamond-like carbon and diamond-like carbon-based nickel nanocomposite films deposited by reactive magnetron sputtering of Ni target," *ACS Appl. Mater. Interfaces*, vol. 10, no. 18, pp. 15778–15785, May 2018, doi: [10.1021/acsami.7b17439](https://doi.org/10.1021/acsami.7b17439).
- [16] M. Petersen, R. Bandorf, G. Bräuer, and C.-P. Klages, "Diamond-like carbon films as piezoresistors in highly sensitive force sensors," *Diamond Rel. Mater.*, vol. 26, pp. 50–54, Jun. 2012, doi: [10.1016/j.diamond.2012.04.004](https://doi.org/10.1016/j.diamond.2012.04.004).
- [17] A. Tibrewala, E. Peiner, R. Bandorf, S. Biehl, and H. Lüthje, "Transport and optical properties of amorphous carbon and hydrogenated amorphous carbon films," *Appl. Surf. Sci.*, vol. 252, no. 15, pp. 5387–5390, May 2006, doi: [10.1016/j.apsusc.2005.12.046](https://doi.org/10.1016/j.apsusc.2005.12.046).
- [18] J. K. Luo, Y. Q. Fu, H. R. Le, J. A. Williams, S. M. Spearing, and W. I. Milne, "Diamond and diamond-like carbon MEMS," *J. Micromech. Microeng.*, vol. 17, no. 7, pp. S147–S163, Jul. 2007, doi: [10.1088/0960-1317/17/7/s12](https://doi.org/10.1088/0960-1317/17/7/s12).
- [19] C.-T. Toh *et al.*, "Synthesis and properties of free-standing monolayer amorphous carbon," *Nature*, vol. 577, no. 7789, pp. 199–203, Jan. 2020, doi: [10.1038/s41586-019-1871-2](https://doi.org/10.1038/s41586-019-1871-2).
- [20] Y. Shen, B. Liao, Z. Zhang, X. Wu, M. Ying, and X. Zhang, "Anti-sand erosion and tribological performance of thick DLC coatings deposited by the filtered cathodic vacuum arc," *Appl. Surf. Sci.*, vol. 533, Dec. 2020, Art. no. 147371, doi: [10.1016/j.apsusc.2020.147371](https://doi.org/10.1016/j.apsusc.2020.147371).
- [21] M. A. Fraga, H. Furlan, R. S. Pessoa, and M. Massi, "Wide bandgap semiconductor thin films for piezoelectric and piezoresistive MEMS sensors applied at high temperatures: An overview," *Microsyst. Technol.*, vol. 20, no. 1, pp. 9–21, Jan. 2014, doi: [10.1007/s00542-013-2029-z](https://doi.org/10.1007/s00542-013-2029-z).
- [22] H. S. Jung, H. H. Park, S. S. Pang, and S. Y. Lee, "The structural and electron field emission characteristics of pulsed laser deposited diamond-like carbon films with thermal treatment," *Thin Solid Films*, vol. 355, pp. 151–156, Nov. 1999, doi: [10.1016/S0040-6090\(99\)00495-2](https://doi.org/10.1016/S0040-6090(99)00495-2).
- [23] J. O. Orwa, I. Andrienko, J. L. Peng, S. Praver, Y. B. Zhang, and S. P. Lau, "Thermally induced sp^2 clustering in tetrahedral amorphous carbon (ta-C) films," *J. Appl. Phys.*, vol. 96, no. 11, pp. 6286–6297, Dec. 2004, doi: [10.1063/1.1808918](https://doi.org/10.1063/1.1808918).
- [24] X. Ma *et al.*, "Piezoresistive behavior of amorphous carbon films for high performance MEMS force sensors," *Appl. Phys. Lett.*, vol. 114, no. 25, Jun. 2019, Art. no. 253502, doi: [10.1063/1.5096225](https://doi.org/10.1063/1.5096225).
- [25] X. Ma *et al.*, "MEMS piezo-resistive force sensor based on DC sputtering deposited amorphous carbon films," *Sens. Actuators A, Phys.*, vol. 303, Mar. 2020, Art. no. 111700, doi: [10.1016/j.sna.2019.111700](https://doi.org/10.1016/j.sna.2019.111700).
- [26] X. Ma, Q. Zhang, P. Guo, X. Tong, Y. Zhao, and A. Wang, "Residual compressive stress enabled 2D-to-3D junction transformation in amorphous carbon films for stretchable strain sensors," *ACS Appl. Mater. Interfaces*, vol. 12, no. 40, pp. 45549–45557, Oct. 2020, doi: [10.1016/acsami.0c12073](https://doi.org/10.1016/acsami.0c12073).
- [27] Š. Meškinis, A. Vasiliauskas, K. Šlapikas, R. Gudaitis, S. Tamulevičius, and G. Niaura, "Piezoresistive properties and structure of hydrogen-free DLC films deposited by DC and pulsed-DC unbalanced magnetron sputtering," *Surf. Coatings Technol.*, vol. 211, pp. 172–175, Oct. 2012, doi: [10.1016/j.surfcoat.2011.10.004](https://doi.org/10.1016/j.surfcoat.2011.10.004).
- [28] I. A. Blech and P. Wood, "Linear thermal expansion coefficient and biaxial elastic modulus of diamondlike carbon films," *J. Vac. Sci. Technol. A, Vac., Surf., Films*, vol. 11, no. 3, pp. 728–729, May 1993, doi: [10.1116/1.578800](https://doi.org/10.1116/1.578800).
- [29] A. J. Bullen, K. E. O'Hara, D. G. Cahill, O. Monteiro, and A. von Keudell, "Thermal conductivity of amorphous carbon thin films," *J. Appl. Phys.*, vol. 88, no. 11, pp. 6317–6320, Dec. 2000, doi: [10.1063/1.1314301](https://doi.org/10.1063/1.1314301).
- [30] M. Hakovirta, J. E. Vuorinen, X. M. He, M. Nastasi, and R. B. Schwarz, "Heat capacity of hydrogenated diamond-like carbon films," *Appl. Phys. Lett.*, vol. 77, no. 15, pp. 2340–2342, Oct. 2000, doi: [10.1063/1.1290387](https://doi.org/10.1063/1.1290387).
- [31] G.-E. Chang, C.-O. Chang, and H. H. Cheng, "Strain analysis of a wrinkled SiGe bilayer thin film," *J. Appl. Phys.*, vol. 111, no. 3, Feb. 2012, Art. no. 034314, doi: [10.1063/1.3682769](https://doi.org/10.1063/1.3682769).
- [32] X. Tong *et al.*, "Micro pressure sensors based on ultra-thin amorphous carbon film as both sensitive and structural components," in *Proc. IEEE SENSORS*, Oct. 2019, pp. 1–4.
- [33] S. Debroy, S. Sivasubramani, G. Vaidya, S. G. Acharyya, and A. Acharyya, "Temperature and size effect on the electrical properties of monolayer graphene based interconnects for next generation MQCA based nanoelectronics," *Sci. Rep.*, vol. 10, no. 1, Apr. 2020, Art. no. 6240, doi: [10.1038/s41598-020-63360-6](https://doi.org/10.1038/s41598-020-63360-6).
- [34] A. K. Yadav *et al.*, "Vertically aligned few-layered graphene-based non-cryogenic bolometer," *C*, vol. 5, no. 2, p. 23, May 2019, doi: [10.3390/c5020023](https://doi.org/10.3390/c5020023).
- [35] Y. Li *et al.*, "Study on the stability of the electrical connection of high-temperature pressure sensor based on the piezoresistive effect of P-type SiC," *Micromachines*, vol. 12, no. 2, p. 216, Feb. 2021, doi: [10.3390/mi12020216](https://doi.org/10.3390/mi12020216).
- [36] A. R. M. Faisal *et al.*, "3C-SiC on glass: An ideal platform for temperature sensors under visible light illumination," *RSC Adv.*, vol. 6, no. 90, pp. 87124–87127, 2016, doi: [10.1039/c6ra19418d](https://doi.org/10.1039/c6ra19418d).
- [37] S. Vinayak, H. P. Vyas, K. Muraleedharan, and V. D. Vankar, "Ni-Cr thin film resistor fabrication for GaAs monolithic microwave integrated circuits," *Thin Solid Films*, vol. 514, nos. 1–2, pp. 52–57, Aug. 2006, doi: [10.1016/j.tsf.2006.02.025](https://doi.org/10.1016/j.tsf.2006.02.025).
- [38] A. A. S. Mohammed, W. A. Moussa, and E. Lou, "Development and experimental evaluation of a novel piezoresistive MEMS strain sensor," *IEEE Sensors J.*, vol. 11, no. 10, pp. 2220–2232, Oct. 2011, doi: [10.1109/jsen.2011.2113374](https://doi.org/10.1109/jsen.2011.2113374).
- [39] S. Tamulevičius *et al.*, "Piezoresistive properties of amorphous carbon based nanocomposite thin films deposited by plasma assisted methods," *Thin Solid Films*, vol. 538, pp. 78–84, Jul. 2013, doi: [10.1016/j.tsf.2012.11.122](https://doi.org/10.1016/j.tsf.2012.11.122).
- [40] R. Koppert, D. Goettel, O. Freitag-Weber, and G. Schultes, "Nickel containing diamond like carbon thin films," *Solid State Sci.*, vol. 11, no. 10, pp. 1797–1800, Oct. 2009, doi: [10.1016/j.solidstatesciences.2009.04.022](https://doi.org/10.1016/j.solidstatesciences.2009.04.022).
- [41] T. Takagi, T. Takeno, and H. Miki, "Metal-containing diamond-like carbon coating as a smart sensor," in *Thermec 2009* (Materials Science Forum), vols. 638–642, T. Chandra, N. Wanderka, W. Reimers, and M. Ionescu, Eds. Switzerland: Trans Tech Publications, 2010, pp. 2103–2108.

- [42] P. Song *et al.*, "A novel piezoresistive MEMS pressure sensors based on temporary bonding technology," *Sensors*, vol. 20, no. 2, p. 337, Jan. 2020, doi: [10.3390/s20020337](https://doi.org/10.3390/s20020337).
- [43] J. Wang, R. Chuai, L. Yang, and Q. Dai, "A surface micromachined pressure sensor based on polysilicon nanofilm piezoresistors," *Sens. Actuators A, Phys.*, vol. 228, pp. 75–81, Jun. 2015, doi: [10.1016/j.sna.2015.03.008](https://doi.org/10.1016/j.sna.2015.03.008).



Xin Ma received the bachelor's degree in mechanical engineering from Xi'an Jiaotong University, China, in 2016. He is pursuing the Ph.D. degree with the Zhao Yulong's Group. His interests include piezo-resistive mechanism of diamond like carbon film and piezo-resistive MEMS sensors.



Qi Zhang received the Ph.D. degree in mechanical engineering from Xi'an Jiaotong University, China, in 2014. Now, she is a Teacher at Xi'an Jiaotong University. Her research interests include the MEMS sensors and piezo-resistive mechanism of new materials, such as graphene and a-C film.



Peng Guo received the Ph.D. degree in materials physics and chemistry from the University of Chinese Academy of Sciences, China, in 2015. Now, he is an Associate Professor with the Ningbo Institute of Materials Technology and Engineering, Chinese Academy of Sciences. His research interests include preparation, characterization, and electrical properties of amorphous carbon films.



Hao Li received the B.S. degree in chemistry from Nankai University in 2015 and the M.E. degree in materials engineering from Tianjin Normal University in 2018. He is pursuing the Ph.D. degree with the Ningbo Institute of Materials Technology and Engineering, Chinese Academy of Sciences. His research interests include amorphous carbon films, electrochemical science, and proton exchange membrane fuel cells.



Yulong Zhao received the Ph.D. degree in mechanical engineering from Xi'an Jiaotong University, China, in 2003. Now, he is a Professor at Xi'an Jiaotong University, where he is an Associate Director of the State Key Laboratory for Manufacturing Systems Engineering. His research interests include MEMS sensors and micro and nano fabrication.



Aiying Wang received the B.S. degree in material science and engineering from Northwestern Polytechnical University, Xi'an, China, in 1998, and the Ph.D. degree from the Institute of Metal Research, Chinese Academy of Sciences, Shenyang, China, in 2003. Her current research interests include advanced carbon-based materials, materials simulation, and plasma surface engineering.